AGU100 ADVANCING EARTH AND SPACE SCIENCE

Geophysical Research Letters

RESEARCH LETTER
10.1029/2020GL087360

Key Points:
- Existing models on the future size of irrigated areas overlook basic parametric and structural uncertainties
- These uncertainties make the potential extension of irrigation in 2050 to be much larger than previously suggested
- The uncertainty in the prediction of future irrigated areas is mostly irreducible

Supporting Information:
- Supporting Information S1
- Text S1

Correspondence to:
A. Puy,
apuy@princeton.edu

Citation:
Puy, A., Lo Piano, S., & Saltelli, A. (2020). Current models underestimate future irrigated areas. *Geophysical Research Letters*, *47*, e2020GL087360. https://doi.org/10.1029/2020GL087360

Received 2 FEB 2020
Accepted 5 APR 2020
Accepted article online 17 APR 2020

Current Models Underestimate Future Irrigated Areas

A. Puy[1,2], S. Lo Piano[3], and A. Saltelli[2,4]

[1]Department of Ecology and Evolutionary Biology, Princeton University, Princeton, NJ, USA, [2]Centre for the Study of the Sciences and the Humanities (SVT), University of Bergen, Bergen, Norway, [3]School of the Built Environment, University of Reading, Reading, UK, [4]Open Evidence Research, Universitat Oberta de Catalunya (UOC), Barcelona, Spain

Abstract Predictions of global irrigated areas are widely used to guide strategies that aim to secure environmental welfare and manage climate change. Here we show that these predictions, which range between 240 and 450 million hectares (Mha), underestimate the potential extension of irrigation by ignoring basic parametric and model uncertainties. We found that the probability distribution of global irrigated areas in 2050 spans almost half an order of magnitude (~300–800 Mha, $P_{2.5}$, $P_{97.5}$), with the right tail pushing values to up to ~1,800 Mha. This uncertainty is mostly irreducible as it is largely caused by either population-related parameters or the assumptions behind the model design. Model end-users and policy makers should acknowledge that irrigated areas are likely to grow much more than previously thought in order to avoid underestimating potential environmental costs.

1. Introduction

The size of irrigated areas is a key parameter defining the social-ecological impact of irrigated agriculture, the most intensive agricultural regime in terms of labour and production per surface unit (Boserup, 1965): It determines crop yields (Dillon, 2011; Netting, 1993),water consumption (Wisser et al., 2008; Puy et al., 2017), the impact of agriculture on global warming (IPCC, 2014), the sustainability of river systems (De Graaf et al., 2019), the spread of water-borne or air-borne diseases (through large-scale flood and sprinkler irrigation respectively FAO, 1997), or rainfall patterns in and around irrigated areas (Alter et al., 2015; Cook et al., 2011). This explains why modeling future irrigated areas is paramount to guide midterm policies on water and biomass demand and to prevent environmental deterioration, poverty and climate change (Hejazi et al., 2014; Shen et al., 2008).

To date, projections of the global irrigated area suggest that it will increase linearly, reaching between 250 and 450 Mha by 2050 (Alcamo et al., 2007, 2005; Alexandratos & Bruinsma, 2012; Fischer et al., 2007; Molden, 2007; Rosegrant et al., 2002; Shiklomanov & Rodda, 2003) (Figure S1 in the supporting information). The narrow range of these predictions raises a fundamental question: Are models of future irrigated areas robust, or do they neglect crucial uncertainties?

Here we address this query and conduct a systematic uncertainty and global sensitivity analysis of the projection of continental and global irrigated areas for 2050. Following previous works (Alcamo et al., 2007, 2005; Alexandratos & Bruinsma, 2012; Fischer et al., 2007; Molden, 2007; Rosegrant et al., 2002; Shiklomanov & Rodda, 2003), we model continental irrigated areas as a function of population, cropland, and water available for irrigation. We keep our model as simple as possible to facilitate its assessment, and unlike previous approaches, we map the model output back onto the projection's main parametric and structural uncertainties Finally, we discuss the nature of these uncertainties, and reflect on the implications of our results for all estimations that use the future extension of irrigation as a model input.

2. Materials and Methods

2.1. The Model

Population is a major constrain of agricultural systems and has been widely used as a driver to project irrigation-related variables in many modeling exercises (Alexandratos & Bruinsma, 2012; Boserup, 1965; Shen et al., 2008; Shiklomanov & Rodda, 2003). We used population size rather than population density to model irrigated areas because it better explains changes in irrigated areas at the continental level (Figures S2 and S3). Although irrigated areas might be conditioned by other factors (i.e., trans-oceanic food

demands and trade networks), the available data suggests that their effective influence is effectively summarized by population size, a parameter that encapsulates many complex features of social-ecological systems (Bettencourt, 2013; Oka et al., 2017; Puy, 2018).

We described the relation between irrigated areas and population with the following equation:

$$\log(Y) = \log(\alpha) + \beta \log(N) \tag{1}$$

where Y and N are respectively irrigated area and population size, α is a constant, and β the scaling exponent describing the growth rate between population size and irrigated area. In order to ground the model on current continental estimates of irrigated areas, we described α as

$$\alpha = \frac{Y_0}{N_0^{\beta}} \tag{2}$$

where Y_0 and N_0 are the irrigated area and the population size at the baseline year $t = 0$.

The world population has been growing super-exponentially for most of known human history, and it has begun to slow down only recently (Johansen & Sornette, 2001). The United Nations (2017) projects this deceleration in population growth rates up to 2100. However, we considered this slowdown uncertain based on the fact that the United Nations has been revising their projections, both upwards and downwards, since 2013, and the intrinsic unpredictability that characterize population dynamics (Pison, 2019). We assumed that some fluctuations in population growth/decline rates should be expected and modeled population growth as

$$\frac{dN}{dt} = rN^{\gamma} \tag{3}$$

where r reflects population growth rate and γ is an exponent that controls the speed of population growth/decline.

Our final model is the result of rearranging equations (1)–(3) (see Text S1 in the supporting information for a step-by-step description):

$$Y = \frac{Y_0}{N_0^{\beta}} \left[N_0^{(1-\gamma)} + rt(1-\gamma) \right]^{\frac{\beta}{(1-\gamma)}} \tag{4}$$

Equation (4) implies that the growth rate of irrigated areas is open ended. This concurs with recent evidence that suggests that continental irrigated areas, on average, grow super-exponentially for a given increase in population (Puy, 2018). However, it can be argued that the expansion of irrigated agriculture is constrained by the availability of cropland and water for irrigation. Such premise draws from the ecological concept of "carrying capacity" the idea of a static boundary that limits how much of a given thing can exist in a given environment (Chapman & Byron, 2018). Although technological innovations to save land and water (i.e., vertical agriculture, Despommier, 2011, or seawater desalination, Burn et al., 2015) have shown this boundary to be dynamic, we acknowledge the implausibility of (1) irrigated areas increasing from the current ~6% to beyond 100% of the arable land in 30 years' time and (2) irrigated areas consuming all freshwater available, as this would leave no water for industrial or domestic use. We thus limited the growth of irrigated areas as follows:

$$f(x) = \begin{cases} Y & Y < K \\ K & \text{otherwise} \end{cases} \tag{5}$$

where $f(x)$ is our new model, Y comes from equation (4), and K is the maximum cropland available.

In order to operationalize water constraints, we began by modeling the relation between the water required for irrigation and the irrigated area as

$$\log(w) = \phi + \delta \log(Y) \tag{6}$$

where w is the volume of water required to irrigate the area Y, ϕ the intercept, and δ the slope of the line of best fit (Figure S4). We then limited the growth of the irrigated area by the maximum volume of water available for irrigation, which we made a fraction of the total water available: If the amount of water required

Table 1
Summary of the Parameters/Triggers and Their Distribution

Param./trigger	Description	Distribution
Y_0	Irrigated area baseline value	$\mathcal{U}(a_j, b_j)$
r	Population growth rate	see SI
γ	Pace of population growth	$\mathcal{N}(1, 0.02)$
t	Baseline year	$\mathcal{DU}(38, 51)$
K	Cropland available	$\mathcal{U}(a_j, b_j)$
W_a	Water available	$\mathcal{U}(a_j, b_j)$
η	Proportion of W_a for irrigation	$\mathcal{U}(0.2, 0.5)$
X_1	Irrigated area data set to compute β	$\mathcal{DU}(1, 6)$
X_2	OLS or SMA regressions for β	$\mathcal{DU}(1, 2)$
X_3	Robust/nonrobust regressions for β	$\mathcal{DU}(1, 2)$
X_4	True value of β	$\mathcal{DU}(1, 10^4)$
W_1	Irrigated area data set to compute (ϕ, δ)	$\mathcal{DU}(1, 6)$
W_3	Robust/nonrobust regressions for (ϕ, δ)	$\mathcal{DU}(1, 2)$
W_4	True value of (ϕ, δ)	$\mathcal{DU}(1, 10^4)$

Note. DU stands for discrete uniform and j is the index of the continent. The rationale behind the selection of the probability distributions is explained in the supporting information. Tables S1–S4 show the specific distributions used for Y_0, r, K, and W_a in each continent j.

to irrigate the area Y is smaller than the total water that can be allocated to irrigation, we keep Y as the model output. Otherwise, the largest area that can be irrigated with the total water available for irrigation is used as the model output:

$$f(x) = \begin{cases} Y & w < W_a\eta \\ \left(\frac{W_a\eta}{10^{\phi}}\right)^{(1/\delta)} & \text{otherwise} \end{cases} \tag{7}$$

where $f(x)$ is our new model, Y comes from equation (4), W_a is the total water available, and η is the proportion of W_a that is allocated to irrigation.

Altogether, our model includes seven uncertain parameters (Table 1). Text S2 in the supporting information justifies their characterization as uncertain and describes the steps taken to mathematically formalize this uncertainty.

2.2. The Triggers

Models also embed structural uncertainties, that is, alternative model formulations might be plausible, and parameters can be computed using a range of different yet equally reasonable approaches (Saltelli et al., 2008). This is the case of β in equation (1) and of (ϕ, δ) in equation (6). To tackle these model uncertainties, we made β and (ϕ, δ) a function of triggers, $\beta = f(X_1, X_2, X_3, X_4)$ and $(\phi, \delta) = f(W_1, W_3, W_4)$. The rationale is the following:

- (X_1, W_1): There are currently six data sets on global irrigated areas (Meier et al., 2018; Thenkabail et al., 2009; Siebert et al., 2013; Salmon et al., 2015; FAO, 2016; FAO, 2017). The values provided by these data sets might differ by up to 4 orders of magnitude at the national level (Figures S5–S7). These different estimations introduce uncertainty in the value of Y in equations (1) and (6), and in consequence, in the calculation of β and (ϕ, δ). X_1 and W_1 were thus used to select which of the six irrigated area data sets should be chosen for the computation of β and (ϕ, δ).
- X_2: β in equation (1) can be computed via ordinary least squares (OLS) or standard major axis (SMA) regressions. OLS would allocate all equation error to Y (i.e., it assumes there is an independent and a dependent variable), whereas SMA would split it into N and Y (i.e., it does not differentiate between the driver and the response variable) (Smith, 2009; Warton et al., 2006). The use of OLS thus implicitly endorses Boserup, 's (1965) model, in which population drives the adoption of intensive agricultural systems, whereas SMA is more appropriate if both variables are considered to be inextricably intertwined

(Morrison, 1994). X_2 was therefore used to decide whether OLS or SMA regressions should be used in equation (1).

- (X_3, W_3). OLS and SMA might provide different estimations of the line of best fit depending on whether robust or nonrobust methods are used. We could confirm the presence of bivariate outliers affecting the computation of α and β and (ϕ, δ) (Figures S8 and S9). X_3 and W_3 were thus used to select whether to apply robust or nonrobust methods for the estimation of β and (ϕ, δ), respectively.
- (X_4, W_4). Even if the aforementioned triggers account for the uncertainty in the computation of β and (ϕ, δ), there still would be uncertainty with regard to their true value. This can be approached by bootstrapping β (ϕ, δ) n times in each of the 24 (12) possible scenarios created by the triggers, thus creating 24 (12) different vectors of β (ϕ, δ) with length n per continent. X_4 and W_4 were therefore used to decide which β and (ϕ, δ) values should be extracted from the vector and used in the computation of equation (4).

2.3. Uncertainty and Sensitivity Analysis

In order to analyze how the model parameters and triggers convey uncertainty to the prediction of irrigated areas, we propagated uncertainty from the inputs to the output. Sobol' quasi-random number sequences were used to generate a $(2^{15}, 2k)$ matrix for each continent (Bratley & Fox, 1988), with k being the number of model parameters plus triggers. The first k-matrix was labeled **A** and the remaining k-matrix, **B**. We allocated each parameter and trigger to a different column and described them using probability distributions according to the continent and the available data (Text S2 and Table 1).

Our model ran rowwise in both the **A** and **B** matrices, as follows: For $v = 1, 2, \ldots, 2^{15}$ rows, it retrieved a $\beta^{(v)}, (\phi^{(v)}, \delta^{(v)})$ value following the conditions set by $X_1^{(v)}$ $(W_1^{(v)})$, $X_2^{(v)}$, $X_3^{(v)}$ $(W_3^{(v)})$, and $X_4^{(v)}$ $(W_4^{(v)})$ and computed equation (4) to obtain $Y^{(v)}$.

To examine which parameters and triggers conveyed the most uncertainty to the model output, we relied on Sobol' indices. We constructed k additional matrices $\mathbf{A}_\mathbf{B}^{(i)}$, $i = 1, 2, \ldots, k$ parameters, where the ith matrix is composed of all columns of the **A** matrix except the ith, which comes from the **B** matrix. Sobol' indices decompose the model output variance (V_Y) as the sum of all conditional variances up to the kth order, as

$$V_Y = \sum_{i=1}^{k} V_i + \sum_{i} \sum_{i<j} V_{ij} + \ldots + V_{1,2,\ldots,k} \tag{8}$$

where V_i is the first-order variance contribution of the ith parameter, V_{ij} the second-order contribution of the interaction between the ith and the jth parameter, and so on up to the kth order. The first-order effect, or the proportion of variance contributed by the ith parameter, is then calculated as

$$S_i = \frac{V_i}{V_Y} \tag{9}$$

We also computed the total-order effect (S_{Ti}), which reflects the proportion of variance contributed by the first-order effect of the ith parameter plus its interactions with all the rest:

$$S_{Ti} = 1 - \frac{V_{\sim i}}{V_Y} \tag{10}$$

The larger the difference between S_{Ti} and S_i, the more the parameter is involved in interactions. Here we used Saltelli et al.'s (2010) and Jansen's (1999) estimators to compute S_i and S_{Ti}, respectively.

In order to ensure the robustness of the results, all the steps taken during our analysis have been replicated independently by two of the coauthors (A. P. and S. L. P.) using two different programming languages and scripts (*R* and *Python*, respectively). The code and all data sets required to replicate our results are publicly available in Zenodo (Lo Piano, 2020; Puy, 2020).

3. Results

3.1. Uncertainty Analysis

Figure 1 shows the empirical distribution of irrigated areas in 2050, Y in equation (4). To compare our results with the projections currently available, Table 2 presents the proportion of model runs yielding $min \leq Y \leq max$ and $Y \geq max$, with *min* and *max* being the minimum and maximum extension of irrigation in 2050,

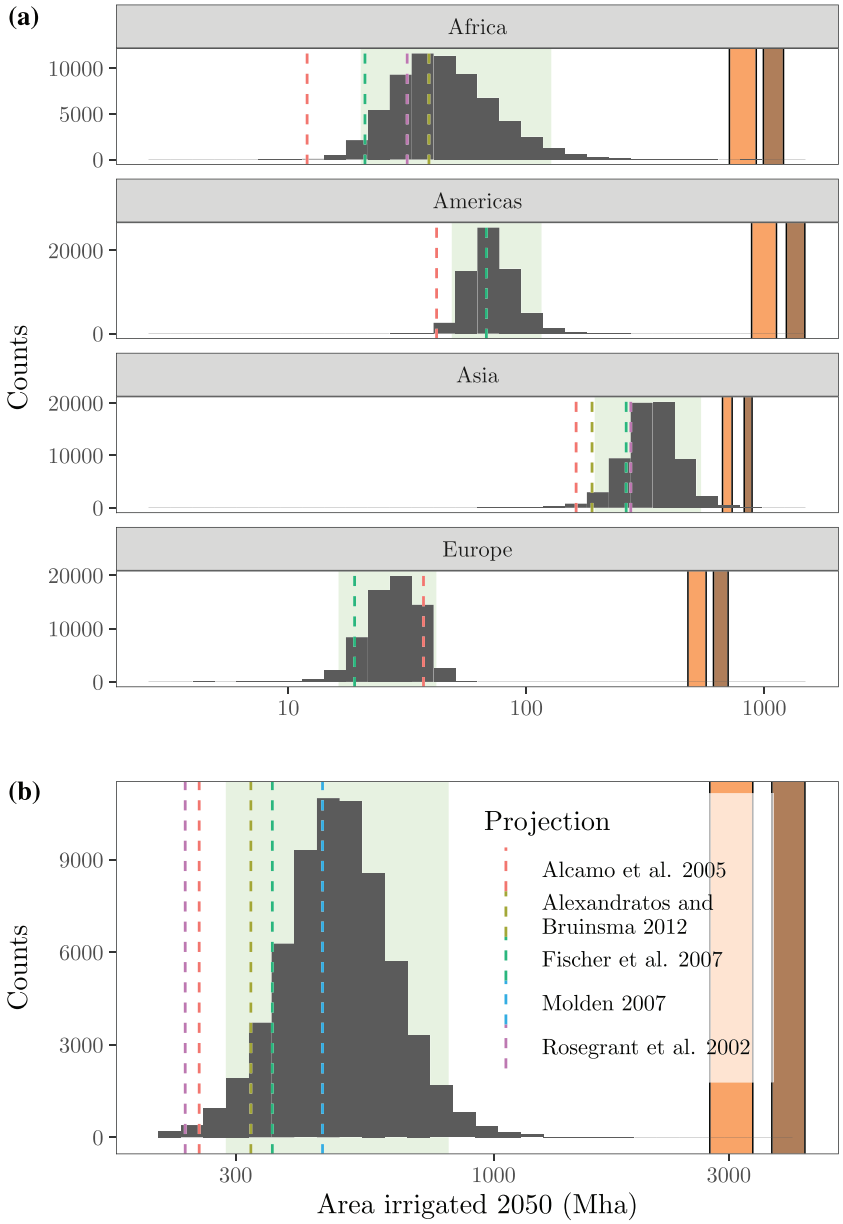

Figure 1. Uncertainty in the projection of irrigated areas to 2050 (the estimation by Rosegrant et al., 2002 is for 2025). The green, transparent rectangle shows the 2.5th and the 97.5th percentiles of the model output distribution. The colored, dotted vertical lines reflect the extension of future continental and global irrigated areas as predicted by previous works. The orange and brown vertical frames show the uncertainty in the net and gross cropland available in 2050, calculated after Zhang and Cai (2011) (Text S2 in the supporting information). (a) Uncertainty at the continental level. (b) Uncertainty at the global level.

as suggested by existing reports (Alcamo et al., 2007, 2005; Alexandratos & Bruinsma, 2012; Fischer et al., 2007; Molden, 2007; Rosegrant et al., 2002; Shiklomanov & Rodda, 2003) (Table S5).

The distribution of the projection of continental irrigated areas significantly overshoots previous estimates, which makes the likelihood of an extreme value much larger than previously suggested (Figure 1a). This is especially the case for the irrigated area of Africa, whose range of possible sizes spans more than one order of magnitude (~20–130 Mha; $P_{2.5}, P_{97.5}$). If we take into account the full empirical distribution, we observe that 60% of our model runs are beyond the maximum extension of irrigation proposed so far for that continent (39 Mha) (Alexandratos & Bruinsma, 2012), and 2% over the 135 Mha which are potentially irrigable according to Xie et al.'s (2014) updated land estimates.

Table 2
Comparison Between Our Model Output Y and the Minimum and Maximum Extensions of Irrigation Proposed by Previous Works

Continent	$min \leq Y \leq max$ (%)	$Y \geq max$ (%)
Africa	40	59
Americas	42	56
Asia	19	80
Europe	80	12

Note. The proportion of model runs yielding $Y \leq min$ is not shown.

In the Americas, Asia, and Europe the potential increase is also significant (~48–120, ~190–550, and ~15–40 Mha, respectively; $P_{2.5}, P_{97.5}$). These values are unevenly constrained by the minimum and maximum extensions reported by existing works (19–80%; Table 2). The uncertainty in the projection for the Americas, Asia and Europe increases to 320, 880, and 63 Mha, respectively, if the upper 2.5% of the distribution is taken into account. In the case of Asia, 15% of our model runs also yielded values as large as K, suggesting significant chances of irrigated agriculture extending over all available cropland by 2050 (Zhang & Cai, 2011). Europe is the only continent with a significant proportion of model runs (~8%) where $Y < min$, indicating that European irrigated areas could actually shrink as a result of a negative population growth rate.

To know how uncertainty at the continental level translates at the global level, we generated a set of row vectors with the model output for the continent j in the vth row. We then calculated the global irrigated area in 2050 as $Y = \sum_{v=1}^{n} Y_j^{(v)}$ (Figure 1b). The range of possible extensions, which is bounded between 300 and 800 Mha ($P_{2.5}, P_{97.5}$), increases to ~1,800 Mha if the right tail of the distribution is taken into account. Our results suggest that there are ~100% and 95% chances of global irrigated areas in 2050 being larger than Alcamo et al.'s (2005) (262 Mha) and FAO's (322 Mha) predictions (Alexandratos & Bruinsma, 2012), and 60% chances of irrigated areas being larger than the largest extension proposed to date (450 Mha) (Molden, 2007). In fact, a scenario where global irrigated areas extend over an area at least twice that size cannot be ruled out (~1%).

Since the expansion of irrigation in our model is driven by population growth (see equation (3)), we checked whether our irrigated area estimates were caused by unreasonably high population values. Instead, the results indicate that the 2.5th to 97.5th percentiles are consistently associated with modeled population sizes bounded by the United Nations' lowest and highest population estimates for 2050 (Figure S10).

3.2. Sensitivity Analysis

Figures 2 and S11–S14 present the results of the sensitivity analysis. We found that the parameters that model water (η, W_a) and cropland (K) availability, as well as the different statistical frameworks available to model how water withdrawals scale with irrigated areas (W_1, W_3), do not contribute any significant uncertainty to the projection of irrigated areas in any continent. Unless the other uncertainties are not reduced, they can be excluded from future models or fixed at any value within their uncertainty range without significantly affecting the projection (Figure 2a).

The other parameters are influential and their importance varies depending on the continent. Europe is the region most influenced by the first-order effect of the irrigated area baseline value Y_0, which explains 55% of the uncertainty in the projection. For countries such as Slovakia or Belgium, the uncertainty in the extension of irrigated agriculture spans three to four orders of magnitude (Figure S7). If reducing the model output variance for Europe is a priority, then efforts should be invested in improving the mapping of irrigated areas. This might be achieved by increasing the accuracy of state-of-the-art measuring tools, such as remote sensing techniques; by reaching an agreement on what exactly is an irrigated area; or by better merging the data compiled in official reports with that obtained from satellite imagery (FAO, 2016, 2017; Meier et al., 2018; Salmon et al., 2015; Siebert et al., 2013; Thenkabail et al., 2009).

The reduction of the projection uncertainty for the other continents is more problematic: First, because a significant proportion of the model output uncertainty for Asia (~65%) and the Americas (~70%) is caused by

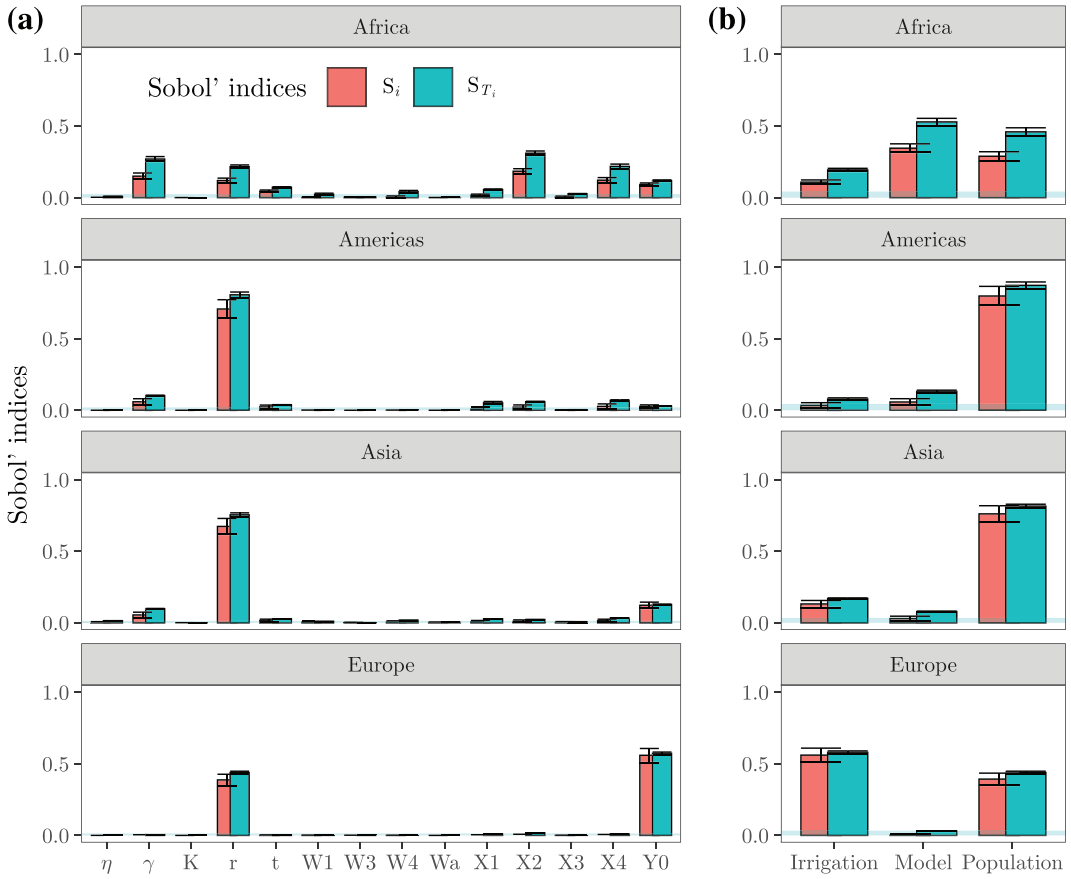

Figure 2. Sobol' indices. S_i and S_{Ti} refer respectively to Sobol' first- and total-order indices. S_i measures the influence of a parameter in the model output, while S_{Ti} measures the influence of a parameter jointly with its interactions. The blue, transparent horizontal frame indicates the approximation error in the calculation of the S_{Ti} indices, S^*_{Ti}. Only S_{Ti} whose lower 95% confidence interval does not overlap with S^*_{Ti} are considered truly influential (see supporting information). (a) Model parameters/triggers (b) Clusters of parameters/triggers: irrigation ($X1, Y_0, W_1, W_a, \eta$), model (X_2, X_3, X_4, W_3, W_4), and population (r, γ). See Table 1 and Text S2 in the supporting information for a description of the parameters.

the population growth rate r, an index largely driven by unpredictable factors such as demographic stochasticity (i.e., randomness in birth/death rates and sex determination) or demographic heterogeneity (i.e., variance in the features affecting survival and reproduction) (Melbourne & Hastings, 2008). Second, because in the case of Africa, it also largely results from the different model structures available ($S_{X_2} + S_{X_4} \approx 30\%$), which is harder to pin down with our current knowledge.

To gain further insight into the structure of the model output uncertainty, we clustered the parameters and the triggers in three groups and simultaneously assessed the uncertainty driven by irrigation, population and model-related inputs (Figure 2b). We observed that the model is largely additive for the Americas, Asia, and Europe: 88–94% of the output uncertainty is explained by the sum of first-order effects, which are dominated by population-related uncertainties in the case of the Americas and Asia and by irrigation-related uncertainties in the case of Europe. The model is nonadditive for Africa (74%), meaning that ~25% of the model output variance results from the interactions between at least two different clusters.

4. Discussion and Conclusions

Irrigation models are widely used to define policies on water and food security, environmental sustainability, and climate change. Their reliability strongly depends on whether their inferences hold once the chain of assumptions they embed is allowed to vary within reasonable bounds. In this paper we provide an understandable, transparent model of future irrigated areas, and exhaustively explore its behavior by activating

the main sources of uncertainty in the assumptions underlying the analysis. Our study aligns with existing works and guidelines that regard the study of uncertainty as an unavoidable step to judge the quality of model-based inferences (Eker et al., 2018; Funtowicz & Ravetz, 1990; Jakeman et al., 2006; van der Sluijs et al., 2004).

Our estimates improve existing ones in several ways. First, in model parsimony and transparency: our projection, which assumes that the growth of irrigated areas is a function of population size limited by future water and cropland availability, is summarized in a one-liner equation that can be readily reviewed. Furthermore, the model output holds against its main underlying parametric (7) and structural (7) uncertainties (Table 1). Information on model dimensionality, mathematical formalization or uncertainty assessment is lacking in previous projections (Alcamo et al., 2007, 2005; Alexandratos & Bruinsma, 2012; Fischer et al., 2007; Molden, 2007; Rosegrant et al., 2002; Shiklomanov & Rodda, 2003), making it hard to assess their robustness.

Although a systematic account is beyond the scope of this study, the evidence suggests that previous models might have indeed left several structural and parametric uncertainties unchecked. For instance, Alcamo et al.'s (2007) or OECD's (2012) proposal of a null increase of irrigated areas assumes the exhaustion of available cropland, the intensification of rainfed agriculture, increases in crop yields, and optimization of world trade. Shiklomanov and Rodda (2003) and Shen et al. (2008), in contrast, assume that past trends in population and irrigated area will continue in the future within the limits of available cropland . These two opposing narratives reflect alternative ways of framing the projection, a setting which can only be dealt with in the context of a stringent uncertainty and sensitivity analysis. Even basic model inputs such as current irrigated areas and future cropland available are treated by previous models as known parameters, despite strong evidence indicating otherwise (Meier et al., 2018; Zhang & Cai, 2011).

Second, our exercise provides a probabilistic estimation of future irrigated areas given the uncertainties involved in the models designed with this purpose. Our results indicate that current estimates are unreliable and should not be used to guide policies on irrigation. By overlooking uncertainties, previous studies failed to detect the considerable weight of the right tail of the output distributions, which can only be accounted for with a global sensitivity analysis (Saltelli et al., 2008). Varying all uncertainties simultaneously is especially important when the model under study is nonadditive (i.e., when it includes multiplications, exponents, etc). This is the case with the model presented in equation (4) and is likely to hold true also for any model projecting irrigated areas as a function of population. As a practitioner of sensitivity analysis would expect, the results of a modeling exercise then tend to exceed what one would envision from the linear mindset, leading to “surprises” (Taleb, 2007).

Third, our work characterizes for the first time the uncertainty involved in projecting irrigated areas. Figure 2 shows that it is mostly additive and yet it might not be easily reduced. In the case of the Americas, Asia, and Europe it is largely driven by the systemic unpredictability that characterises population dynamics, which might be hard to pin down. Even if a fertility-constraining policy is globally implemented, its effects might not be felt until way past 2050, suggesting that there are no easy ways to change the broad population trends (Bradshaw & Brook, 2014). Large-scale population control measures implemented without understanding the underlying demographical regime might also have unwelcomed and counterintuitive consequences (i.e., higher birth rates, as in India in the early 1950s; see Connelly, 2008). In the case of Africa, which presents a larger contribution of nonadditivities, canceling out the stochasticity in population dynamics would not make the projection of irrigated areas less sensitive to model uncertainties. This renders the addition of extra mathematical complexity unlikely to increase the accuracy of the model should all the parametric and structural uncertainty of the addition be also taken into account.

By casting a long shadow on the robustness of current predictions on irrigated areas, our results also loom large over all the studies that rely on these estimates to model any related variable or environmental phenomenon. This includes not only projections on irrigation water withdrawals (Alcamo et al., 2007; Döll & Siebert, 2002; Wada et al., 2016; Wisser et al., 2008) or CO_2 emissions (Chaturvedi et al., 2013) but also models on climate change. As a direct effect, it has been demonstrated that the extent of irrigation affects the amount of water vapor in the atmosphere and surface temperature (Boucher et al., 2004). Higher-order effects might include an increase in albedo and shortwave reflection (Cook et al., 2015) or the modification of downwind and cloud formation processes (Lo & Famiglietti, 2013), potentially affecting very remote regions

(De Vrese et al., 2016). Without accounting for the wide distribution of future irrigated areas, any modeling exercise focused on projecting irrigation-related variables risks to dramatically minimize, or directly ignore, the latent environmental impact of irrigated agriculture.

Acknowledgments
This work has been funded by the European Commission (Marie Skłodowska-Curie Global Fellowship, Grant 792178 to A. P.). The code and all data sets required to replicate our results are available in Zenodo (Lo Piano, 2020; Puy, 2020). The outputs of our study, including the sample matrix and the distributions of irrigated areas in 2050, are available in PANGAEA at https://doi.pangaea.de/10.1594/PANGAEA.914665.

References

Alcamo, J., Döll, P., Henrichs, T., Kaspar, F., Lehner, B., Rösch, T., & Siebert, S. (2003). Global estimates of water withdrawals and availability under current and future "business-as-usual" conditions. *Hydrological Sciences Journal*, *48*(3), 339–348. https://doi.org/10.1623/hysj.48.3.339.45278

Alcamo, J., Flörke, M., & Märker, M. (2007). Future long-term changes in global water resources driven by socio-economic and climatic changes. *Hydrological Sciences Journal*, *52*(2), 247–275. https://doi.org/10.1623/hysj.52.2.247

Alcamo, J., Van Vuuren, D., Cramer, W., Alder, J., Bennett, E., Carpenter, S., et al. (2005). Changes in ecosystem goods and services and their drivers across the scenarios. In S. Carpenter, P. Pingali, E. Bennett, & M. Zurek (Eds.), *Scenarios of the millennium ecosystem assessment* (pp. 297–373). Oxford: Island Press.

Alexandratos, N., & Bruinsma, J. (2012). World agriculture towards 2030/2050. The 2012 revision: Rome: FAO. https://doi.org/10.1016/S0264-8377(03)00047-4

Alter, R. E., Im, E. S., & Eltahir, E. A. B. (2015). Rainfall consistently enhanced around the Gezira Scheme in East Africa due to irrigation. *Nature Geoscience*, *8*(10), 763–767. https://doi.org/10.1038/ngeo2514

Bettencourt, L. M. A. (2013). The origins of scaling in cities. *Science*, *340*(6139), 1438–1441. https://doi.org/10.1126/science.1235823

Boserup, E. (1965). *The conditions of agricultural growth*. London: George Allen 6 Unwin Ltd.

Boucher, O., Myhre, G., & Myhre, A. (2004). Direct human influence of irrigation on atmospheric water vapour and climate. *Climate Dynamics*, *22*(6-7), 597–603.

Bradshaw, C. J. A., & Brook, B. W. (2014). Human population reduction is not a quick fix for environmental problems. *Proceedings of the National Academy of Sciences*, *111*(46), 16,610–16,615. https://doi.org/10.1073/pnas.1410465111

Bratley, P., & Fox, B. L. (1988). ALGORITHM 659: Implementing Sobol's quasirandom sequence generator. *ACM Transactions on Mathematical Software (TOMS)*, *14*(1), 88–100.

Burn, S., Hoang, M., Zarzo, D., Olewniak, F., Campos, E., Bolto, B., & Barron, O. (2015). Desalination techniques—A review of the opportunities for desalination in agriculture. *Desalination*, *364*, 2–16. https://doi.org/10.1016/j.desal.2015.01.041

Chapman, E. J., & Byron, C. J. (2018). The flexible application of carrying capacity in ecology. *Global Ecology and Conservation*, *13*, 1–12. https://doi.org/10.1016/j.gecco.2017.e00365

Chaturvedi, V., Hejazi, M., Edmonds, J., Clarke, L., Kyle, P., Davies, E., & Wise, M. (2013). Climate mitigation policy implications for global irrigation water demand. *Mitigation and Adaptation Strategies for Global Change*, *20*(3), 389–407. https://doi.org/10.1007/s11027-013-9497-4

Connelly, M. (2008). *Fatal misconception: The struggle to control world population*, (Vol. 26). Cambridge, MA: Harvard University Press. https://doi.org/10.1080/07341511003629606

Cook, B. I., Puma, M. J., & Krakauer, N. Y. (2011). Irrigation induced surface cooling in the context of modern and increased greenhouse gas forcing. *Climate Dynamics*, *37*(7-8), 1587–1600. https://doi.org/10.1007/s00382-010-0932-x

Cook, B. I., Shukla, S. P., Puma, M. J., & Nazarenko, L. S. (2015). Irrigation as an historical climate forcing. *Climate Dynamics*, *44*(5-6), 1715–1730. https://doi.org/10.1007/s00382-014-2204-7

Döll, P., & Siebert, S. (2002). Global modeling of irrigation water requirements. *Water Resources Research*, *38*(4), 1037. https://doi.org/10.1029/2001WR000355

Damkjaer, S., & Taylor, R. (2017). The measurement of water scarcity: Defining a meaningful indicator. *Ambio*, *46*(5), 513–531. https://doi.org/10.1007/s13280-017-0912-z

De Graaf, I. E. M., Gleeson, T., (Rens) van Beek, L. P. H., Sutanudjaja, E. H., & Bierkens, M. F. P. (2019). Environmental flow limits to global groundwater pumping. *Nature*, *574*(7776), 90–94. https://doi.org/10.1038/s41586-019-1594-4

De Vrese, P., Hagemann, S., & Claussen, M. (2016). Asian irrigation, African rain: Remote impacts of irrigation. *Geophysical Research Letters*, *43*, 3737–3745. https://doi.org/10.1002/2016GL068146

Despommier, D. (2011). The vertical farm: Controlled environment agriculture carried out in tall buildings would create greater food safety and security for large urban populations. *Journal fur Verbraucherschutz und Lebensmittelsicherheit*, *6*(2), 233–236. https://doi.org/10.1007/s00003-010-0654-3

Dillon, A. (2011). Do differences in the scale of irrigation projects generate different impacts on poverty and production?. *Journal of Agricultural Economics*, *62*(2), 474–492. https://doi.org/10.1111/j.1477-9552.2010.00276.x

Eker, S., Rovenskaya, E., Obersteiner, M., & Langan, S. (2018). Practice and perspectives in the validation of resource management models. *Nature Communications*, *9*(1), 1–10. https://doi.org/10.1038/s41467-018-07811-9

FAO (1997). *Irrigation potential in Africa. A basin approach*. Rome: FAO Land and Water Development Division. Retrieved from http://www.fao.org/3/w4347e/w4347e00.htm

FAO (2016). AQUASTAT website. Rome. Retrieved from http://www.fao.org/nr/water/aquastat/didyouknow/index3.stm

FAO (2017). FAOSTAT database. Rome:Food and Agriculture Organization of the United Nations. Retrieved from http://www.fao.org/faostat/en/

Filzmoser, P., Garrett, R. G., & Reimann, C. (2005). Multivariate outlier detection in exploration geochemistry. *Computers and Geosciences*, *31*(5), 579–587. https://doi.org/10.1016/j.cageo.2004.11.013

Fischer, G., Tubiello, F. N., van Velthuizen, H., & Wiberg, D. A. (2007). Climate change impacts on irrigation water requirements: Effects of mitigation, 1990-2080. *Technological Forecasting and Social Change*, *74*(7), 1083–1107. https://doi.org/10.1016/j.techfore.2006.05.021

Funtowicz, S. O., & Ravetz, J. R. (1990). *Uncertainty and quality in science for policy*. Dordrecht: Kluwer Academic Publishers.

Hejazi, M., Edmonds, J., Clarke, L., Kyle, P., Davies, E., Chaturvedi, V., et al. (2014). Long-term global water projections using six socioeconomic scenarios in an integrated assessment modeling framework. *Technological Forecasting and Social Change*, *81*(1), 205–226. https://doi.org/10.1016/j.techfore.2013.05.006

IPCC (2014). *Climate change 2014: Mitigation of climate change. Contribution of Working Group III to the Fifth Assessment report of the Intergovernmental Panel on Climate Change*. Cambridge and New York: Cambridge University Press.

Jakeman, A. J., Letcher, R. A., & Norton, J. P. (2006). Ten iterative steps in development and evaluation of environmental models. *Environmental Modelling & Software*, *21*(5), 602–614. https://doi.org/10.1016/j.envsoft.2006.01.004

Jansen, M. (1999). Analysis of variance designs for model output. *Computer Physics Communications*, *117*(1-2), 35–43. https://doi.org/10.1016/S0010-4655(98)00154-4

Johansen, A., & Sornette, D. (2001). Finite-time singularity in the dynamics of the world population, economic and financial indices. *Physica A: Statistical Mechanics and its Applications*, *294*(3-4), 465–502. https://doi.org/10.1016/S0378-4371(01)00105-4

Lincoln Simon, J. (2014). *Population and development in poor countries: Selected essays*. Princeton: Princeton Legacy Library.

Lo, M.-H., & Famiglietti, J. S. (2013). Irrigation in California's Central Valley strengthens the southwestern U.S. water cycle. *Geophysical Research Letters*, *40*, 301–306. https://doi.org/10.1002/grl.50108

Lo Piano, S. (2020). *Confareneoclassico/irrigation_model: Irrigated areas—Python implementation*: Zenodo. https://doi.org/10.5281/zenodo.3726558

Meier, J., Zabel, F., & Mauser, W. (2018). A global approach to estimate irrigated areas. A comparison between different data and statistics. *Hydrology and Earth System Sciences*, *22*(2), 1119–1133. https://doi.org/10.5194/hess-22-1119-2018

Melbourne, B. A., & Hastings, A. (2008). Extinction risk depends strongly on factors contributing to stochasticity. *Nature*, *454*(7200), 100–103. https://doi.org/10.1038/nature06922

Molden, D. (Ed.) (2007). *Water for food, water for life: A comprehensive assessment of water management in agriculture Edited by* Molden, D. London: Earthscan, and Colombo: International Water Management Institute. https://doi.org/10.1007/s10795-008-9044-8

Morrison, K. D. (1994). The intensification of production: Archaeological approaches. *Journal of Archaeological Method and Theory*, *1*(2), 111–159. https://doi.org/10.1007/BF02231414

Netting, R. M. (1993). *Smallholders, householders. Farm families and the ecology of intensive, sustainable agriculture*. Stanford: Stanford University Press.

OECD (2012). Water. In OECD (Ed.), *Environmental outlook to 2050: The consequences of inaction* (pp. 275–332): OECD Publishing. https://doi.org/10.1787/9789264122246-en

Oka, R. C., Kissel, M., Golitko, M., Sheridan, S. G., Kim, N. C., & Fuentes, A. (2017). Population is the main driver of war group size and conflict casualties. *Proceedings of the National Academy of Sciences*, *114*(52), E11101–E11110. https://doi.org/10.1073/pnas.1713972114

Pison, G. (2019). How many humans tomorrow? The United Nations revises its projections. Retrieved 2019-12-17, from http://theconversation.com/how-many-humans-tomorrow-the-united-nations-revises-its-projections-118938

Puy, A. (2018). Irrigated areas grow faster than the population. *Ecological Applications*, *28*(6), 1413–1419. https://doi.org/10.1002/eap.1743

Puy, A. (2020). *R code of the paper "Current models underestimate future irrigated areas"*: Zenodo. https://doi.org/10.5281/zenodo.3725874

Puy, A., Muneepeerakul, R., & Balbo, A. L. (2017). Size and stochasticity in irrigated social-ecological systems. *Scientific Reports*, *7*, 43,943. https://doi.org/10.1038/srep43943

Rosegrant, M. W., Cai, X., & Cline, S. (2002). World water and food to 2025: Dealing with scarcity. Retrieved from http://www.ifpri.org/sites/default/files/publications/water2025.pdf https://doi.org/10.1098/rstb.2005.1744

Salibián-Barrera, M., Van Aelst, S., & Willems, G. (2008). Fast and robust bootstrap. *Statistical Methods and Applications*, *17*(1), 41–71. https://doi.org/10.1007/s10260-007-0048-6

Salmon, J. M., Friedl, M. A., Frolking, S., Wisser, D., & Douglas, E. M. (2015). Global rain-fed, irrigated, and paddy croplands: A new high resolution map derived from remote sensing, crop inventories and climate data. *International Journal of Applied Earth Observation and Geoinformation*, *38*, 321–334. https://doi.org/10.1016/j.jag.2015.01.014

Saltelli, A., Annoni, P., Azzini, I., Campolongo, F., Ratto, M., & Tarantola, S. (2010). Variance based sensitivity analysis of model output. Design and estimator for the total sensitivity index. *Computer Physics Communications*, *181*(2), 259–270. https://doi.org/10.1016/j.cpc.2009.09.018

Saltelli, A., Ratto, M., Andres, T., Campolongo, F., Cariboni, J., Gatelli, D., et al. (2008). *Global sensitivity analysis. The primer*. Chichester, UK: John Wiley. https://doi.org/10.1002/9780470725184

Shen, Y., Oki, T., Utsumi, N., Kanae, S., & Hanasaki, N. (2008). Projection of future world water resources under SRES scenarios: Water withdrawal. *Hydrological Sciences*, *53*(1), 11–33. https://doi.org/10.1623/hysj.53.1.11

Shiklomanov, I. A., & Rodda, J. C. (2003). *World water resources at the beginning of the 21st century*. Cambridge: Cambridge University Press.

Siebert, S., Henrich, V., Frenken, K., & Burke, J. (2013). *Update of the digital global map of irrigation areas to version 5*. Rome: Food and Agriculture Organization of the United Nations.

Smith, R. J. (2009). Use and misuse of the reduced major axis for line-fitting. *American Journal of Physical Anthropology*, *140*(3), 476–486. https://doi.org/10.1002/ajpa.21090

Taleb, N. (2007). *The Black Swan. The impact of the highly improbable*. New York: Random House.

Thenkabail, P. S., Biradar, C. M., Noojipady, P., Dheeravath, V., Li, Y., Velpuri, M., et al. (2009). Global Irrigated Area Map (GIAM), derived from remote sensing, for the end of the last millennium. *International Journal of Remote Sensing*, *30*(14), 3679–3733. https://doi.org/10.1080/01431160802698919

United Nations (2017). World population prospects: The 2017 revision. Retrieved from https://population.un.org/wpp/

van der Sluijs, J. P., Risbey, J., Kloprogge, P., Ravetz, J. R., Funtowicz, S. O., Corral, S., et al. (2004). RIVM/MNP Guidance for uncertainty assessment and communication: Tool catalogue for uncertainty Assessment (*Tech. Rep. No. October 2003*). Retrieved from https://www.feem-web.it/nostrum/db_doc/RIVM_MNP_2004.pdf

Wada, Y., Flörke, M., Hanasaki, N., Eisner, S., Fischer, G., Tramberend, S., et al. (2016). Modeling global water use for the 21st century: The Water Futures and Solutions (WFaS) initiative and its approaches. *Geoscientific Model Development*, *9*(1), 175–222. https://doi.org/10.5194/gmd-9-175-2016

Warton, D. I., Duursma, R. A., Falster, D. S., & Taskinen, S. (2012). smatr 3—An R package for estimation and inference about allometric lines. *Methods in Ecology and Evolution*, *3*(2), 257–259. https://doi.org/10.1111/j.2041-210X.2011.00153.x

Warton, D. I., Wright, I. J., Falster, D. S., & Westoby, M. (2006). Bivariate line-fitting methods for allometry. *Biological Reviews*, *81*(2), 259. https://doi.org/10.1017/S1464793106007007

Wisser, D., Frolking, S., Douglas, E. M., Fekete, B. M., Vörösmarty, C. J., & Schumann, A. H. (2008). Global irrigation water demand: Variability and uncertainties arising from agricultural and climate data sets. *Geophysical Research Letters*, *35*, L24408. https://doi.org/10.1029/2008GL035296

Xie, H., You, L., Wielgosz, B., & Ringler, C. (2014). Estimating the potential for expanding smallholder irrigation in Sub-Saharan Africa. *Agricultural Water Management*, *131*, 183–193. https://doi.org/10.1016/j.agwat.2013.08.011

Zhang, X., & Cai, X. (2011). Climate change impacts on global agricultural land availability. *Environmental Research Letters*, *6*(1), 14,014. https://doi.org/10.1088/1748-9326/6/1/014014